

# High-Throughput Trace-Level Suspect Screening for Per- and Polyfluoroalkyl Substances in Environmental Waters by Peak-Focusing Online Solid Phase Extraction and High-Resolution Mass Spectrometry

Gordon J. Getzinger\* and P. Lee Ferguson\*

Cite This: <https://doi.org/10.1021/acsestwater.0c00309>

Read Online

ACCESS |



Metrics &amp; More



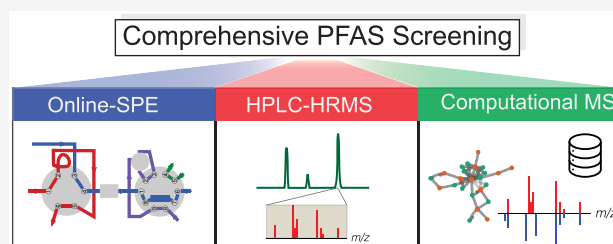
Article Recommendations



Supporting Information

**ABSTRACT:** Per- and polyfluoroalkyl substances (PFASs) occur widely in environmental waters. PFAS risk assessment necessitates the identification of unanticipated PFASs at trace levels and therefore requires determinative methods with nanogram per liter detection limits and the ability to provide detailed molecular and structural information for nontargeted molecules. High-resolution mass spectrometry (HRMS) enables comprehensive PFAS characterization but is currently limited by low-throughput sample preparation techniques that are prone to interference and analyte losses due to sample handling and manual mass spectral interpretation approaches. Here we report the development of a peak-focusing, online solid phase extraction–HRMS method for suspect screening analysis of PFASs in environmental waters. The realized method utilized 6 mL of sample and required <40 min of instrument time for extraction and HRMS analysis. Method evaluation using 45 model PFASs revealed typical method detection limits of 0.1–4 ng L<sup>-1</sup>. The accuracy and precision on repeated analysis of a standard reference material were typically 89–103% and <10%, respectively. A suspect screening approach using an extensive PFAS molecular database and computational mass spectrometry was demonstrated through the analysis of aqueous film-forming foam-impacted surface water samples. Results indicate that the developed methodology is suitable for high-throughput and sensitive molecular annotation of diverse PFASs in environmental waters.

**KEYWORDS:** per- and polyfluoroalkyl substances, high-resolution mass spectrometry, suspect screening, environmental waters, online solid phase extraction, trace analysis



## INTRODUCTION

Per- and polyfluoroalkyl substances (PFASs) make up a class of high-production volume chemicals favored for their unique physicochemical properties.<sup>1</sup> Widespread occurrence of PFASs in the aquatic environment<sup>2</sup> coupled with limited removal by conventional drinking water treatments<sup>3</sup> continues to fuel interest in developing methods for detecting PFASs in environmental waters. Furthermore, routinely monitored PFASs represent a small fraction of PFASs occurring in environmental waters.<sup>4–6</sup> The diversity of PFASs used in commerce, the limited availability of structural information (e.g., structures protected as confidential business information), the potential environmental (bio)chemical transformation of PFASs, and the relative paucity of PFAS analytical standards coupled with their often low concentrations in environmental waters present unique analytical challenges for this compound class. Therefore, to inform PFAS risk assessment, sensitive, high-throughput methods for determining the chemical structure and fate of trace-level, unexpected, or previously unreported PFASs are needed.

PFASs of interest to environmental waters are typically polar and surface-active, making them amenable to detection by atmospheric-pressure ionization (e.g., electrospray or atmospheric-pressure chemical ionization) coupled to mass spectrometry, typically after reversed phase high-performance chromatography (HPLC–MS).<sup>7,8</sup>

HPLC–MS methods utilizing nominal-resolution MS, for instance the triple quadrupole MS instruments common to most quantitative PFAS methods, identify and quantify PFASs using reference standards, which precludes the detection of unexpected or previously unreported PFASs. Therefore, high-resolution mass spectrometry (HRMS), providing accurate mass full-scan and tandem mass spectra, is employed to assign probable structures to unknown PFASs by suspect or nontarget

**Received:** December 24, 2020

**Revised:** April 2, 2021

**Accepted:** April 6, 2021

screening. Screening approaches for PFASs have heretofore focused primarily on using mass defect filtering with subsequent manual structure annotation to assign plausible structures to detected chromatographic features.<sup>9–12</sup> While effective for small sample batches, such approaches are poorly suited to large-scale monitoring studies due to their reliance on user intervention and consequent potential for bias or user errors. A number of computational mass spectrometry tools are available for providing weight of evidence to the tentative identification of organic small molecules detected by HRMS.<sup>13</sup> However, aside from one recent example of a rule-based fragment ion prediction approach,<sup>14</sup> few computational mass spectrometry approaches have been developed for HRMS PFAS analysis. We recently described a comprehensive PFAS molecular database and accompanying *in silico* mass spectral library for the identification of PFASs in environmental samples by HRMS.<sup>15</sup> Here we extend that approach to include environmental occurrence patterns and demonstrate an automated strategy for structure annotation of PFASs in environmental samples.

Samples prepared for HPLC–HRMS PFAS analysis typically require enrichment and cleanup by solid phase extraction (SPE) to achieve sufficient full-scan and tandem HRMS signals for structure annotation of contaminants in the low-nanogram per liter range. For instance, typical sample preparation for HPLC–HRMS analysis utilizes 0.5–1 L of sample concentrated 1000-fold using offline SPE. However, the effective enrichment achieved by offline SPE methods is a function of the initial sample volume, the enrichment factor, and the analytical injection volume.<sup>16</sup> Considering only the analytical step of a method (i.e., injection of a concentrated sample on the chromatographic system), the fraction extracted ( $E$ ) can be defined as the ratio of the on-column mass of the analyte ( $Q_A$ ) to the total mass of the analyte present in the original sample ( $Q'_A$ ).<sup>17</sup> For a lossless offline SPE method that enriches 0.5 L of a 1 ng/L sample to 0.5 mL and injects 10  $\mu$ L on the chromatographic system,  $Q'_A = 500$  pg,  $Q_A = 10$  pg, and  $E = 0.02$ . In contrast,  $E = 1$  for an idealized online SPE method because the entire sample is transferred to the analytical column, while simultaneously requiring smaller sample volumes and less sample handling. Because sample handling and common laboratory materials used in offline SPE methods may contaminate samples or contribute to analyte losses due to accumulation and sorption at air interfaces or to sample containers, such steps inflate method detection limits (MDLs).<sup>18</sup> Furthermore, offline sample preparation techniques are costly, sample intensive, and time-consuming, limiting assay throughput. In contrast, use of online SPE apparatus, such as the one described herein that injects the entirety of a 6 mL environmental water sample, enables large sample enrichments with low sample volume requirements and minimal sample handling and manipulation. Therefore, online SPE provides the preferred approach for achieving the rigorous method requirements of high-throughput HRMS(/MS) PFAS analysis.

Mixed-mode anion exchange reversed phase (AX-RP) extraction is the preferred sorbent method for PFAS enrichment due to the large number of PFASs that are anionic at ambient environmental pH. While several online SPE–HPLC–HRMS methods have been applied for PFAS detection, solvent incompatibilities prevent those methods from applying AX-RP column chemistries.<sup>11,19–22</sup> Furthermore, commonly applied online SPE approaches for PFAS analysis utilize an enrichment strategy in which analytes are extracted at the head of a large particle trapping column and then gradient eluted through the

entire trapping column volume before being transferred to the analytical column, which results in suboptimal sensitivity due to peak broadening. Peak-focusing online SPE circumvents previous challenges in online SPE PFAS analysis by configuration of the online SPE system with a small particle and narrow bore AX-RP trapping column that is front-loaded with sample before back-elution under low-flow, high-solvent strength conditions (i.e., pH >10, 100% organic) and subsequently diluted with a postcolumn makeup flow before being directed to a RP analytical column. Dilution of the trap column eluent postcolumn decreases the solvent strength to achieve peak focusing on the subsequent analytical column, which improves sensitivity by limiting band broadening.

Here we describe development of a peak-focusing, online SPE–HPLC–HRMS instrumental method and an accompanying comprehensive suspect screening workflow for nontargeted detection and formula/structure annotation of trace-level PFASs in environmental waters. The realized method utilizes 6 mL of an environmental water sample, requires only a single centrifugation sample preparation step, and achieves low-nanogram per liter detection limits with an approximately 30 min run time. We establish method analytical figures of merit using PFAS reference standards and certified reference materials and demonstrate method utility in screening analysis of PFAS-impacted surface water samples.

## EXPERIMENTAL SECTION

**Reagents and Materials.** Unless otherwise noted, all solvents were of HPLC grade or better. Nanopure water that had previously been characterized for PFAS background contamination was used to prepare standard solutions. PFAS standards were purchased neat or as prepared standards and were of the highest purity available (see Figure 3 for the structures of model PFASs and Table S1 for a table of compound identifiers and vendors). Methanolic stock and working solutions were stored refrigerated in polypropylene bottles. Reference materials (RM) 8446-Perfluorinated Carboxylic Acids and Perfluorooctance Sulfonamide in Methanol (8446A and 8446B) and 8447-Perfluorinated Sulfonic Acids in Methanol were obtained from the National Institute of Standards and Technology (NIST).

**Sample Preparation.** Immediately prior to analysis, 6 mL of sample was transferred to a 15 mL polypropylene centrifuge tube loaded with 7.5 pg of mass-labeled internal standards (see Table S1 for a list of isotope-labeled internal standards) in 6 mL of methanol. Samples were centrifuged for 30 min (4300 rpm, 4 °C) before 11 mL was decanted into a glass autosampler vial with magnetic metal screw caps (Thermo Scientific).

**Chromatography.** The online SPE system consisted of a robotic autosampler (CTC PAL, CTC Analytics AG) equipped with two six-port two-position high-pressure actuator valves and one ten-port two-position high-pressure actuator valve, a side-port syringe with a 10 mL dilutor module, three UPLC pumps (P1, Ultimate LPG-3400RS; P2, Ultimate NCP-3200RS; P3, HPG-3400RS), and a thermostated column compartment (all from ThermoFisher Scientific, San Jose, CA). P1 and P3 were equipped with C<sub>18</sub> trapping columns (P1, Acclaim 120 C<sub>18</sub>, 2.1 mm  $\times$  10 mm, 5  $\mu$ m particle size, Thermo Scientific; P3, Acclaim 120 C<sub>18</sub>, 2.1 mm  $\times$  50 mm, 2.2  $\mu$ m particle size, Thermo Scientific) positioned immediately after their respective gradient mixers to capture any background interference originating from fluoropolymers in the UPLC pumps and from background contamination of HPLC solvents. Where possible, all wetted

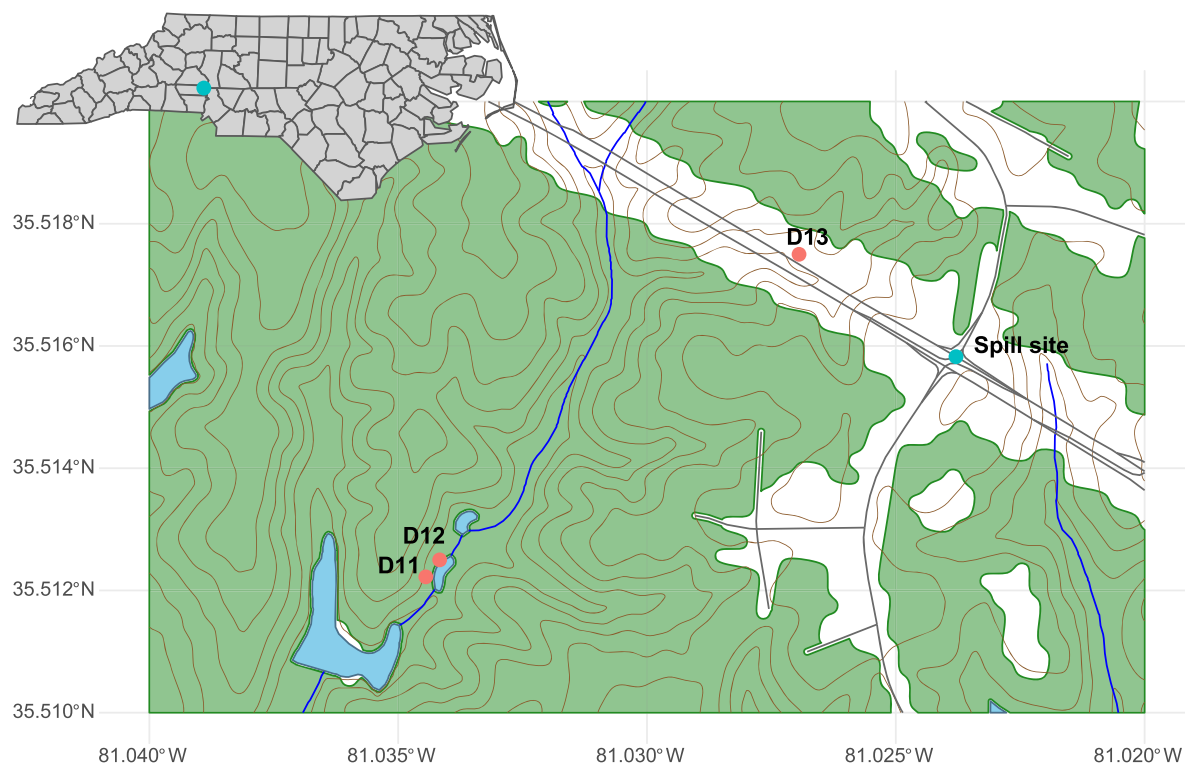


**Figure 1.** Map of spill site and surface water sample locations (D11–D13). Water bodies, flowlines, roadways, and ground surface elevation contours are from the U.S. Geological Survey national hydrography data set.

fluoropolymer materials were replaced with PEEK or stainless steel. Online enrichment/cleanup utilized an Oasis WAX column (2.1 mm × 20 mm, 30 μm, Waters Corp., Ireland), eluted with 2% NH<sub>4</sub>OH in a 1:1 (v/v) methanol/acetonitrile solvent. Analytical chromatography was performed on an Accucore RP-MS column (100 mm × 2.1 mm, 2.6 μm, Thermo Scientific) under gradient elution conditions with water and acetonitrile as eluents. Figure 2 provides a detailed depiction of the online SPE–HPLC apparatus and method program.

**Mass Spectrometry.** HPLC column eluent was directed to a heated electrospray ionization source operated in negative ionization mode (heater temperature, 350 °C; capillary temperature, 250 °C; spray voltage, −2.5 kV; sheath gas, 50 arbitrary units; auxiliary gas, 10 arbitrary units). Mass spectrometry was performed using an Orbitrap Fusion Lumos high-resolution mass spectrometer (Thermo Scientific). Full-scan HRMS data [ $R = 120000$  full width at half-maximum (fwhm) at  $m/z$  200] were acquired from  $m/z$  150 to 2000 with internal lock mass calibration. Data-dependent HRMS<sup>2</sup> data ( $R = 15000$  fwhm at  $m/z$  200) were acquired on quadrupole precursor selected ions with higher-energy collisional dissociation [HCD; stepped collision energies of 20%, 35%, and 50%]. Data-dependent MS<sup>2</sup> (ddMS<sup>2</sup>) utilized a custom-made targeted mass list containing 3506  $m/z$ 's corresponding to known PFAS compounds with molecular weights of 100–2000 Da and at least one hydrogen atom.<sup>15</sup> Detection of an  $m/z$  from the mass list triggered targeted MS/MS analysis; otherwise, the ddMS<sup>2</sup> scan program completed as many scans as possible, in a 1 s cycle time, on nontargeted ions (sorted by intensity). Peak apex detection triggered ddMS<sup>2</sup> when the peak height exceeded 30% of the predicted height based on an expected peak width of 12 s (fwhm).

**Data Processing.** Feature detection and tandem mass spectral library searching were performed using Compound Discoverer (Thermo Scientific, ver. 3.0). Detected features were structurally annotated using a previously reported PFAS structural database and in silico MS/MS library.<sup>15</sup> Predicted MS/MS spectra were precomputed using the Competitive Fragmentation Modeling (CFM) algorithm.<sup>23</sup> Fragment ion trees were generated using the SIRIUS algorithm.<sup>24</sup>

**Trapping Efficiency.** The trapping efficiency of the online SPE system was measured by comparing peaks areas for triplicate analysis of equal mass injections (100 pg on-column) by the realized online SPE method (10 mL injection of a 10 ng L<sup>−1</sup> solution) and by direct injection (20 μL of a 5 μg L<sup>−1</sup> solution).

**Recovery.** Method recovery was determined by replicate ( $N = 6$ ) analysis of NIST RM 8446 and 8447 spiked into nanopure water at approximately 20 ng L<sup>−1</sup> and carried through the entire sample preparation and online SPE analysis.

**Environmental Sample Collection.** Surface water samples were collected near a site where aqueous film-forming foam (AFFF) was applied to extinguish a fuel fire caused by a tanker truck accident that occurred on January 28, 2020 (National Response Center Sequence 1269790). One sample was collected from a drainage ditch approximately 300 m from the spill site. Two additional samples were collected approximately 800 m downstream from where the drainage ditch met an unnamed stream. Figure 1 depicts the spill site and sample locations. Water samples were collected in 15 mL polypropylene conical centrifuge tubes and stored frozen (−20 °C) until preparation and analysis. Subsampling followed the approach described by Backe et al. to minimize losses due to partitioning to surfaces and air–water interfaces.<sup>25</sup>

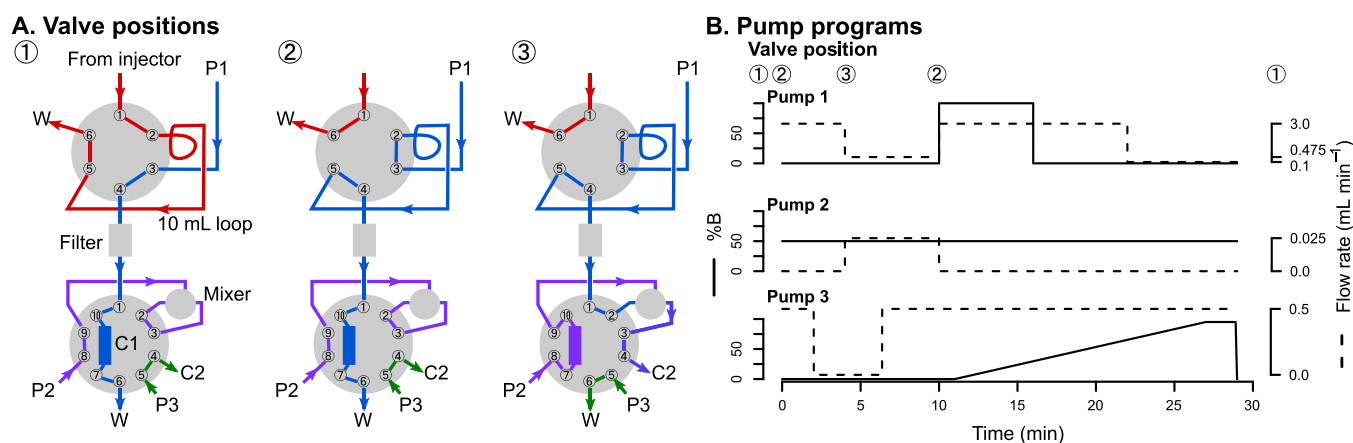


**Figure 2.** (A) Valve positions, pump 1–3 (P1–P3) connections, waste ports (W), trapping (C1), and analytical column (C2) placement for the online SPE system. (B) Programmed flow rates and gradient conditions for P1–P3. During the pre- and postrun segments, valves are at ① allowing low-pressure sample loading via a large-volume syringe into the 10 mL sample loop. At the run start, valves actuate to ② and the sample is loaded at a high flow rate ( $3 \text{ mL min}^{-1}$ ) by P1 through a filter element ( $0.2 \mu\text{m}$ ) onto C1. After C1 had been washed, valves actuate to ③ and C1 is back-eluted with elution buffer at low flow rate ( $25 \mu\text{L min}^{-1}$ ) by P2. Post-C1 eluent combines with dilution/makeup flow from P1 ( $0.475 \text{ mL min}^{-1}$ ) in a high-pressure static mixer to lower the solvent strength and bring the flow rate to  $0.5 \text{ mL min}^{-1}$  before being directed to C2. After elution, valves return to position ② for cleaning and re-equilibration of C1 while C2 is gradient eluted to the mass spectrometer using P3. The following solvent compositions were used: P1, A being 0.1% (v/v) acetic acid in water and B being 2%  $\text{NH}_4\text{OH}$  in a 1:1 methanol/acetonitrile solvent; P2, A and B being 2%  $\text{NH}_4\text{OH}$  in a 1:1 acetonitrile/methanol solvent; P3, A being water and B being acetonitrile.

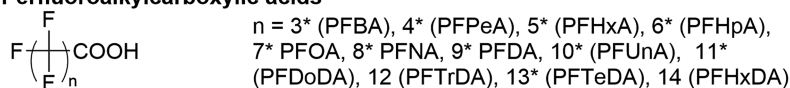
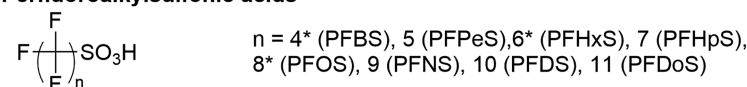
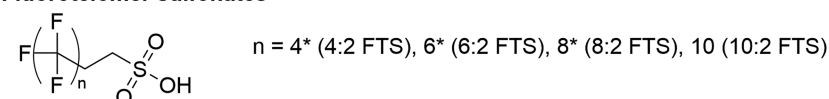
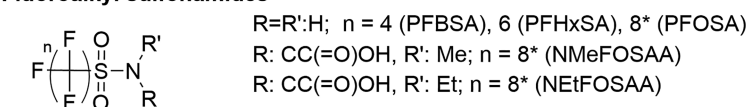
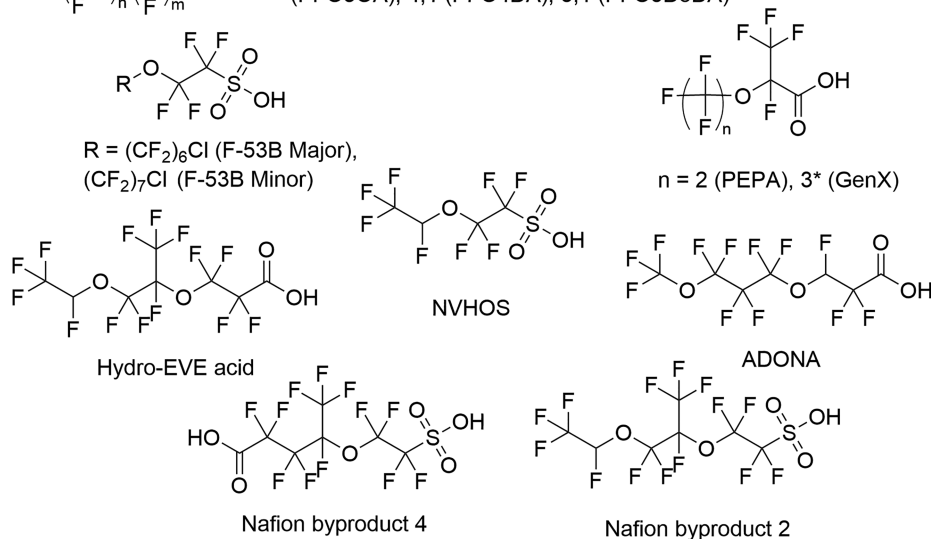
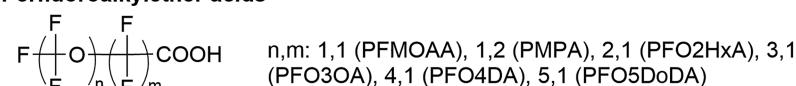
## RESULTS AND DISCUSSION

**Peak-Focusing Online SPE.** Use of a mixed-mode anion exchange reversed phase trapping column enabled enrichment of PFASs with a wide range of physicochemical properties and provided a truly orthogonal approach for sample concentration (via ion exchange) before analyte separation (via reversed phase). Low-molecular weight and highly acidic compounds, such as small perfluoro sulfonic and carboxylic acids, were efficiently trapped utilizing the anion exchange capacity of the Oasis WAX column, while sorption losses (e.g., to vials and transfer lines) for long-chain PFASs were minimized by using 50% methanol as a co-solvent in the autosampler vial. Peak-focusing online SPE enables this approach because anionic analytes must be eluted from anion exchange sorbents with basic solvent and apolar analytes require strong solvents for quantitative transfer from reversed phase sorbents. Under typical online SPE conditions, basic eluents cannot be used, due to incompatibility with silica-based reversed phase column chemistries, and gradient elution with the trapping column in line with the analytical column leads to peak broadening. To overcome these challenges, we utilized a small-volume, 100% organic elution plug containing 2% ammonium hydroxide. To prevent damage to the analytical column caused by a strong base while enabling peak sharpening via flow acceleration post-elution, eluent from the trapping cartridge was diluted in a high-pressure mixing tee with 0.1% acetic acid in water. To further limit peak broadening, the swept volume of the trapping column was minimized by using columns with small particles and capillary transfer lines. In the final configuration, the trapping column was eluted at a rate of  $25 \mu\text{L min}^{-1}$  with a 1:1 (v/v) acetonitrile/methanol solvent containing 2% (v/v) ammonium hydroxide and the makeup flow was 0.1% (v/v) acetic acid in water at a rate of  $475 \mu\text{L min}^{-1}$ , providing optimal trapping and transfer efficiency and suitable chromatographic peak shape for the model PFASs tested. Figure 4 illustrates the sharp chromatographic resolution and high sensitivity obtained for a variety of PFASs analyzed using the peak-focusing online SPE–HRMS method.

Typical offline WAX SPE methods for PFAS implement an organic wash step to elute neutral matrix components that may interfere with PFASs of interest. While this approach is feasible in an online SPE configuration, our approach leveraged the high-performance characteristics of HRMS to limit matrix interference while forgoing the additional wash step. In addition, the ability of the WAX sorbent to trap both neutral and anionic PFASs in this case was a significant advantage for our purposes, as it allowed us to increase the breadth of PFAS compounds that could be detected by our method. Further method refinements might consider including an organic wash step to separate neutral PFASs from anionic PFASs during sample preparation or if a low-resolution mass spectrometer is used for analysis.

**Method Performance.** The peak-focusing online SPE system provided excellent performance characteristics for the analysis of targeted PFASs in environmental water samples. The performance of the method was characterized for five common classes of PFASs, depicted in Figure 3, including perfluoroalkyl ether acids ( $N = 16$ ), perfluoroalkyl carboxylic acids ( $N = 12$ ), fluoroalkyl sulfonamides ( $N = 5$ ), perfluoroalkyl sulfonic acids ( $N = 8$ ), and fluorotelomer sulfonates ( $N = 4$ ). Model PFASs ranged from 180 to 814 Da, contained 5–31 fluorine atoms, and spanned a range of nonfluorinated end-group functionalities. Compound identifiers, including names and registry numbers, for the model PFASs can be found in Table S1, and a summary of method performance for the model compounds can be found in Table 1.

Detection limits for model PFASs were in the range of  $0.05\text{--}2 \text{ ng L}^{-1}$  ( $0.5\text{--}20 \text{ pg on column}$ ) corresponding to  $0.1\text{--}4 \text{ ng L}^{-1}$  for prepared samples. MDLs in the realized method were comparable and at times lower than lowest-concentration minimum reporting levels for EPA methods 533 and 537.1, which enrich 0.25 L of sample using offline SPE and use HPLC–QqQ as the determinative method, demonstrating that the developed method is suitable for trace-level PFAS analysis. Median MDLs were highest for perfluoroalkyl ether acids, which are known to give poor electrospray responses at higher temperatures due to in-source reactions.<sup>19</sup> Further improve-

**Perfluoroalkylcarboxylic acids****Perfluoroalkylsulfonic acids****Fluorotelomer sulfonates****Fluoroalkyl sulfonamides****Perfluoroalkylether acids**

**Figure 3.** Structures of model PFASs used for method development and validation. Asterisks indicate structures with stable isotope-labeled isotopologues used as internal standards. See the [Supporting Information](#) for a complete table of molecular identifiers, suppliers, and structure representations.

ments in MDLs could be achieved by applying separate methods with high- and low-temperature atmospheric pressure ionization conditions (i.e., electrospray heater and ion-inlet capillary temperatures) at the cost of increased sample volume and lower sample throughput incurred by performing two separate analysis. In general, MDLs were well below current PFAS screening levels (e.g., U.S. EPA value of  $70 \text{ ng L}^{-1}$  for PFOA and PFOS), demonstrating that the method was suitable for monitoring PFASs at environmentally relevant concentrations.

Trapping efficiency measures the ability of an online SPE column to enrich analytes from the sample matrix. Because sample loading was decoupled from the analytical column, trapping efficiency strongly influenced method detection limits. We determined trapping efficiency by comparing the relative response of analytes measured under direct injection conditions versus those measured under online SPE conditions. Trapping efficiencies for the model PFAS compounds are listed in [Table 1](#). Under optimized injection programming, the median trapping efficiency was 99.6% and had an interquartile range of 94.6–

107%. These values reflect the broad and robust extraction profile of the applied mixed-mode anion exchange reverse phase online SPE column for PFAS analysis.

Method precision and accuracy were determined by repeated analysis ( $N = 6$ ) of NIST reference materials 8446A, 8446B, and 8447 diluted to a final concentration of approximately  $20 \text{ ng L}^{-1}$ . In total, certified values were available for 15 of the 45 analytes tested in these reference materials. Accuracy ranged from 55.9% to 149.8%, had a median value of 92.7%, and had an interquartile range of 89.4–103.8%. Precision on replicate analysis was typically  $<10\%$ . Recoveries were lowest for short-chain PFASs, likely resulting from the high co-solvent fraction during extraction (i.e., 50% methanol) and thus possibly low trapping efficiency for such compounds on the WAX sorbent. In investigations in which long-chain PFASs are determined to be of little interest, the method presented here may be adapted to improve the recovery of short-chain PFASs by decreasing the co-solvent content of the prepared sample. Results of reference material analysis indicated that the method provided sufficient

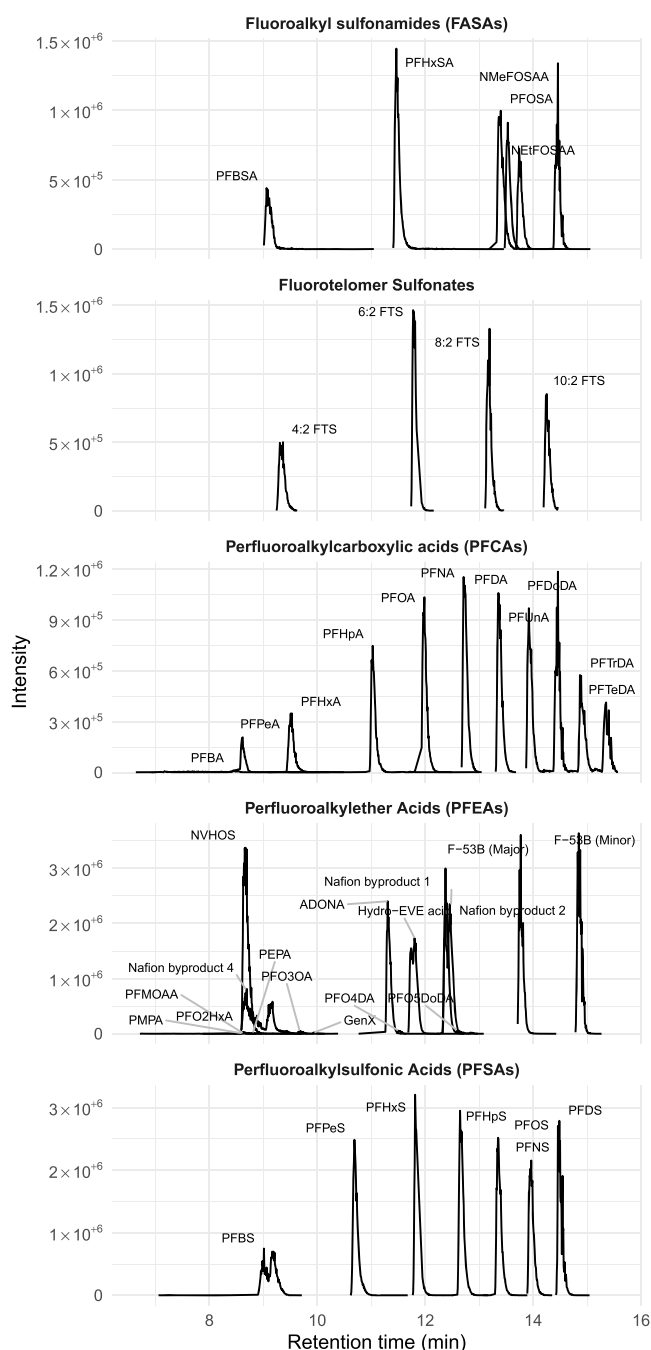


**Figure 4.** Extracted ion chromatograms (XICs) by compound class for  $5 \text{ ng L}^{-1}$  PFASs analyzed by online SPE–HRMS. XICs were constructed using the exact mass of the deprotonated molecular formula (i.e.,  $[M - H]^-$ ) with a 2 ppm mass error window (i.e., exact mass  $\pm 1$  ppm).

reproducibility for qualitative analysis of large batches of environmental samples.

**PFAS Suspect Screening Analysis.** We applied a suspect screening approach combining a comprehensive PFAS structure database and computational mass spectrometry tools to achieve high-throughput PFAS identification from online SPE–HRMS analysis with minimal analyst intervention. The structure database, which is reported in detail elsewhere,<sup>26</sup> contained >60000 PFASs either reported as commercial products or predicted as environmental transformation (i.e., hydrolysis and

**Table 1.** Method Performance for Model PFAS Analytes

compound	trapping efficiency (%) <sup>a</sup>	LOD ( $\text{ng L}^{-1}$ ) <sup>b</sup>	recovery (%) <sup>c</sup>
Perfluoroalkylether Acids			
PFMOAA	$107 \pm 0.7$	2	–
PMPA	$29.7 \pm 14.9$	2	–
PFO2HxA	$139.9 \pm 8.1$	2	–
PEPA	$87.9 \pm 7.8$	2	–
NVHOS	$105.7 \pm 2.9$	0.1	–
PFO3OA	$114.8 \pm 6.6$	0.5	–
GenX	$99.6 \pm 1.3$	0.1	–
PFO4DA	$90.2 \pm 3.2$	0.25	–
Perfluoroalkylcarboxylic Acids			
PFBA	$39.5 \pm 1.7$	2	$56 \pm 28$
PFPeA	$97.3 \pm 1.3$	0.25	$96 \pm 6.4$
PFHxA	$94.6 \pm 0.5$	0.25	$72 \pm 4.9$
PFHpA	$97.6 \pm 0.3$	0.5	$91 \pm 6.2$
PFOA	$98.8 \pm 0.5$	0.1	$96 \pm 6.4$
PFNA	$101.3 \pm 0.2$	0.25	$90 \pm 5.3$
PFDA	$112.3 \pm 0.004$	0.25	$110 \pm 6$
PFUnA	$100 \pm 0.3$	0.1	$88 \pm 6.6$
PFDoDA	$101.8 \pm 2.1$	0.25	$92 \pm 6.2$
PFTrDA	$56 \pm 15.7$	2	$88 \pm 12$
PFTeDA	$100.3 \pm 3.0$	2	$93 \pm 6.2$
PFHxDA	$183.8 \pm 99.2$	1	–
Fluoroalkyl Sulfonamides			
PFBSA	$1.1 \pm 0.1$	0.1	–
PFHxSA	$1.8 \pm 0.02$	0.1	–
PFOSA	$102.4 \pm 1.5$	0.05	$110 \pm 8.1$
NMeFOSAA	$94.6 \pm 0.01$	0.1	–
NETFOSAA	$95.7 \pm 0.2$	0.1	–
ADONA	$98.8 \pm 3.0$	0.1	–
hydro-EVE acid	$138.3 \pm 3.0$	0.1	–
Nafion byproduct 4	$8.3 \pm 0.1$	0.05	–
Nafion byproduct 1	$114.5 \pm 0.1$	0.1	–
PFO5DoDA	$143.5 \pm 3.5$	0.5	–
Nafion byproduct 2	$107.4 \pm 0.4$	0.1	–
F-53B (major)	$94.9 \pm 6.3$	0.1	–
F-53B (minor)	$73.8 \pm 2.1$	0.25	–
Perfluoroalkylsulfonic Acids			
PFBS	$99.4 \pm 0.3$	0.1	$150 \pm 5.2$
PFPeS	$121.5 \pm 4.6$	0.1	–
PFHxS	$103 \pm 0.4$	0.1	$130 \pm 4.8$
PFHpS	$84.4 \pm 0.8$	0.1	–
PFOS	$102.5 \pm 0.1$	0.1	$100 \pm 4.3$
PFNS	$100 \pm 4.2$	0.25	–
PFDS	$77.9 \pm 7.1$	0.25	–
PFDoS	$105.1 \pm 55.7$	0.5	–
Fluorotelomer Sulfonates			
4:2 FTS	$96.8 \pm 0.5$	0.05	–
6:2 FTS	$110.1 \pm 0.4$	0.1	–
8:2 FTS	$111.5 \pm 0.7$	0.25	–
10:2 FTS	$98.8 \pm 7.8$	0.25	–

<sup>a</sup>Average trapping efficiency ( $\pm$ standard deviation). <sup>b</sup>Limit of detection defined as the lowest calibration standard giving <30% RSD for triplicate injections. <sup>c</sup>Recovery ( $\pm$ standard deviation).

biotransformation) products of commercial PFASs. This database also included predicted MS/MS spectra for all PFAS structures. After consolidation and dereplication using Compound Discoverer version 3.0, detected mass spectral features were queried against the PFAS database. Accurate masses, isotope patterns, and fragmentation spectra were considered in

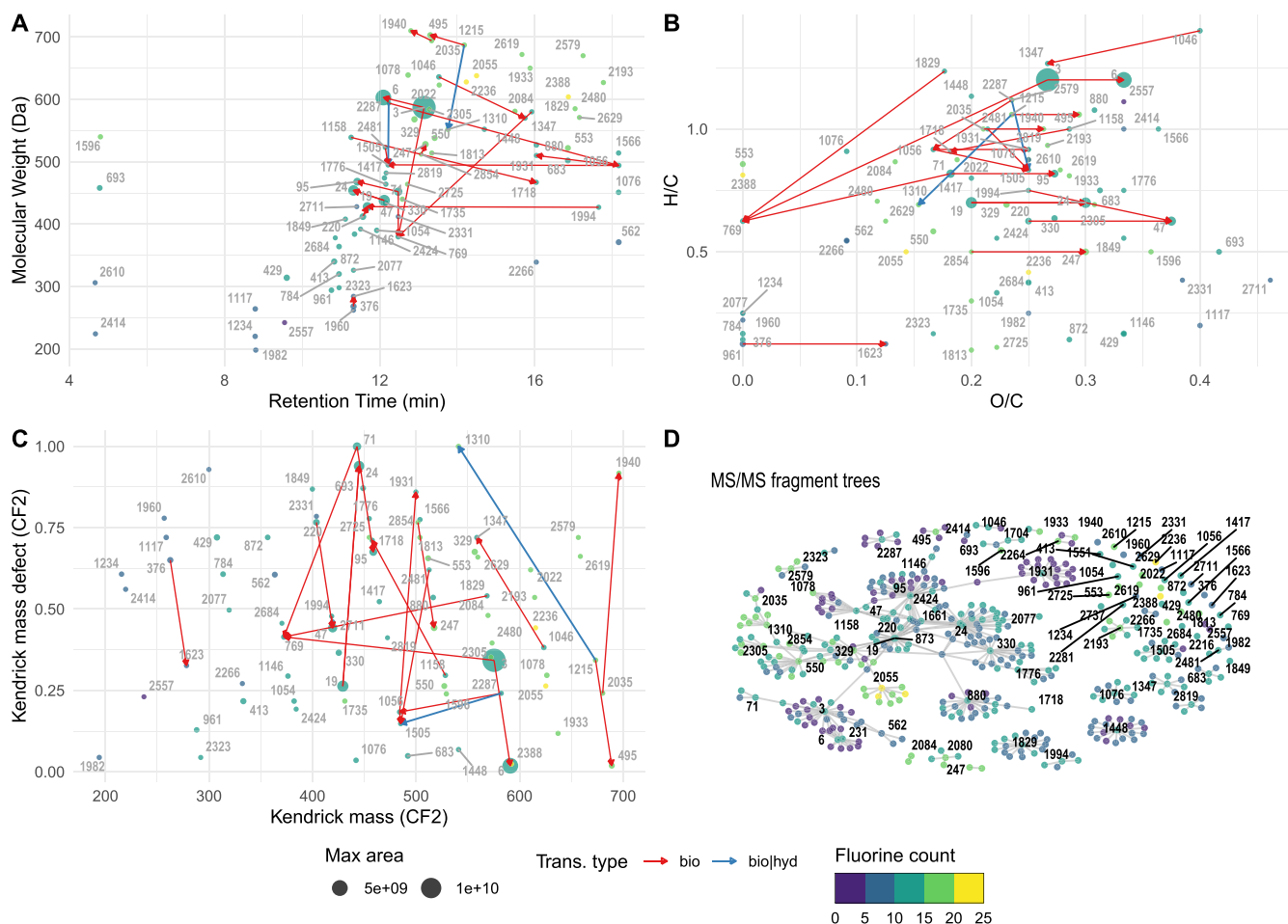


**Figure 5.** Molecular characteristics of putative PFASs detected in surface water samples downstream from an AFFF application. Points are colored according to the number of fluorine atoms in the structure annotation. In panels A–C, point sizes represent the maximum chromatographic peak area of a compound detected in a sample scaled to the area of the compound with the largest peak area in all samples. Points are numbered by rank order maximum peak area in the unfiltered data set (e.g., feature 3 was the feature with the third largest peak area of all detected features). In panels A–C, arrows depict compound relationships from the underlying PFAS molecular database. Predicted biotransformations are depicted with red arrows, while reactions predicted to occur by either biotransformation or hydrolysis are depicted with blue arrows. Panels A–C depict the molecular properties of the detected features and highlight potential relationships between features as revealed through Van Krevelen and Kendrick mass defect space. Panel D shows fragmentation trees for detected features. Numbered nodes represent molecular formulas from features (i.e., intact parent ions), while unnumbered points are fragment molecular formulas annotated by SIRIUS. Connections between points indicate that either a parent formula occurs as a product of another parent or two or more parents share the same fragment molecular formula.

assigning possible molecular elemental and structural formulas. In the absence of analytical standards, several lines of experimental evidence were applied to establish confidence in structure annotations. First, experimental MS/MS spectra were compared to fragment ion trees generated by SIRIUS and *in silico* fragmentation spectra generated by CFM with matched fragment ions providing evidence for plausible molecular and structural formula assignments, respectively. SIRIUS fragmentation tree annotations and CFM-predicted fragment ions were generated for each detected feature and stored in database tables keyed to the detected feature table by feature identifier. Network analysis enabled interrogation and extraction of molecular features linked by shared SIRIUS fragment tree nodes (i.e., fragment ion molecular formula) or CFM-predicted fragment ions (i.e., predicted fragment ion SMILES string). Second, we considered the apparent chemical relationships among detected features. The chemical relationship was determined by predicted parent–product relationships in the underlying PFAS database. Finally, we compared molecular graphs of postulated structures to evaluate for the presence of shared structure motifs using

maximum common substructure analysis. An example of this approach is illustrated in the following description of the analysis of environmental samples.

**Application to Identification of PFASs in AFFF-Impacted Surface Waters.** The developed method was applied to surface water samples collected downstream from an accident site where a fuel fire was extinguished using an AFFF product of unknown composition. Targeted analysis, using the 45 model PFASs as calibration standards, revealed concentrations of 6:2 FTS in the range of 6–46 ng L<sup>-1</sup> and trace levels of several other known PFAS compounds: [PFHxA] = 0.64–1 ng L<sup>-1</sup>, [8:2 FTS] = 0.28–1.1 ng L<sup>-1</sup>, [PFO5DoDA] = 0.5–1.23 ng L<sup>-1</sup>, [GenX] = 0.11–0.23 ng L<sup>-1</sup>, and [PFOA] = 0.11–0.28 ng L<sup>-1</sup>. Employing an HRMS/MS library search strategy—using the mzCloud library, which contains HRMS/MS spectra for more than 17000 compounds—6:2 FTS (87%), 8:2 FTS (89%), 10:2 FTS (78%), PFHxA (89%), PFOA (77%), and PFNA (77%) were annotated as probable structures by spectral matching (parentic values indicate the spectral library match score). Concordance of targeted analysis and library

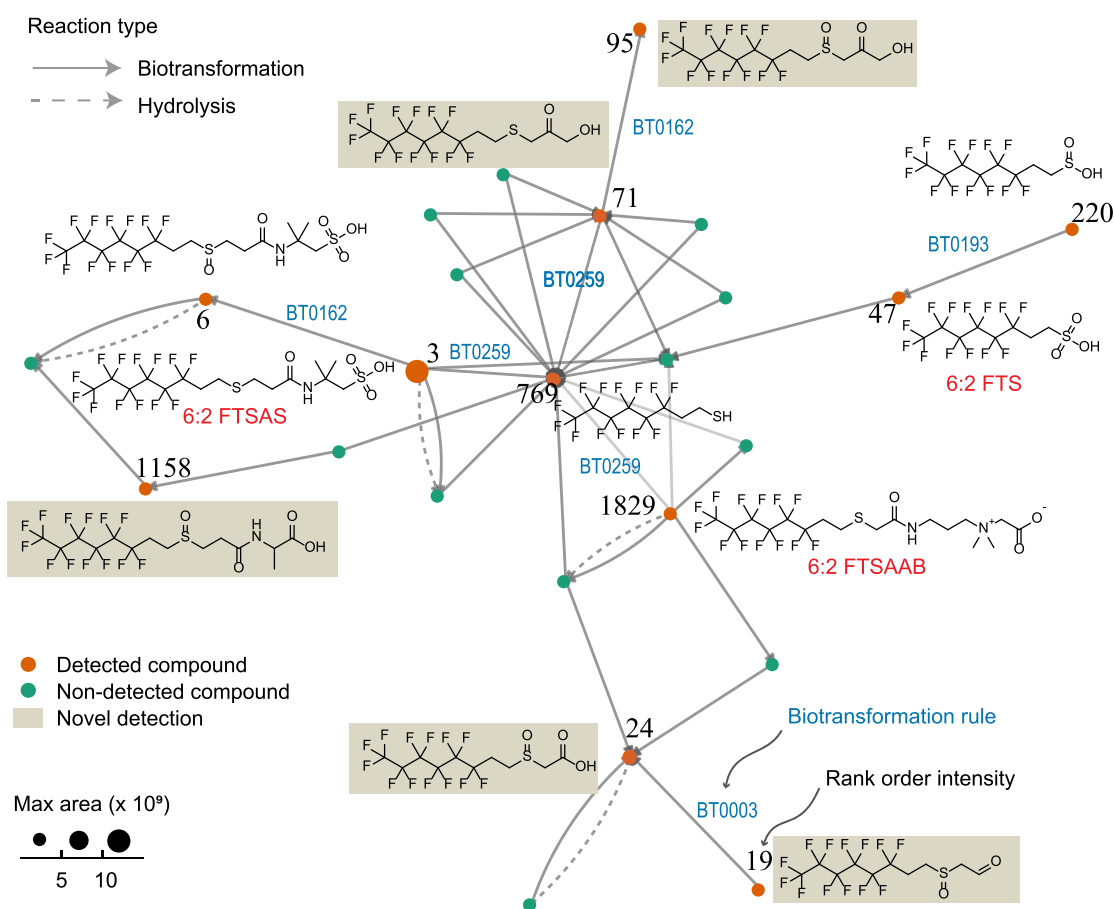


**Figure 6.** Molecular network for compounds detected in surface waters downstream from an AFFF application. See the text for a description of filtering steps. Nodes (i.e., filled circles) represent unique database entries (i.e., PFASs). Nodes are joined by edges (i.e., arrows) that indicate either a predicted hydrolysis (dashed arrows) or biotransformation (solid arrows) reaction. Nodes colored orange indicate those that were detected by HPLC–HRMS, while those in green indicate compounds present in the database but not detected by HPLC–HRMS. Nodes are numbered according to their rank order intensity in the peak table and scaled according to area (undetected nodes are set to the minimum circle size). Representative biotransformation rules are indicated for select transformation and correspond to the EAWAG biotransformation rules associated with that transformation. Highlighted structures indicate those tentatively identified compounds that have not been previously reported to occur in environmental media.

screening reflect the availability of those compounds as analytical standards. However, the dominant PFAS identified by these approaches was 6:2 FTS, which is known to be a degradation product of AFFF products but is not itself an active ingredient in AFFF. These results indicated that the applied AFFF product most likely contained an active ingredient based on 6:2 FTS and that the active ingredient was not a commonly monitored PFAS compound and thus did not occur in either our target analyte panel or a large, well-curated MS/MS library. Therefore, we applied our nontargeted screening approach with the aim of identifying the source AFFF ingredients and any other related compounds.

Feature extraction and annotation were performed on data files from the analysis of the surface water samples and method blanks as described above, resulting in 2917 detected compounds (i.e., unique de-isotoped and de-adducted accurate mass and retention time pairs). Peak areas ( $A$ ) of compounds detected in method blanks ( $A^{\text{blank}}$ ) were compared to those found in unknown samples ( $A^{\text{sample}}$ ), and compounds for which  $A^{\text{blank}}/A^{\text{sample}} > 0$  or  $A^{\text{sample}}/A^{\text{blank}} < 5$  were considered background and totaled 1529. Compounds without MS/MS spectra due to either low intensity or nonselection by the data-dependent analysis algorithm, totaling 928, were marked as such. Compounds marked as background or without MS/MS

spectra, a match within mass error tolerance to our in-house PFAS suspect database, an assigned formula, or a valid *in silico* MS/MS library match were eliminated, resulting in 92 compounds for further consideration.

The molecular properties of the detected compounds, numbered by rank order maximum area in the unfiltered data set, are presented in Figure SA–C, and their associated candidate chemical structures can be found in Table S2. The maximum compound area observed among all samples was assumed to be approximately proportional to concentration and therefore enabled semiquantitative ranking of detected compounds. Putative PFAS compounds had neutral molecular weights in the range of approximately 200–700 Da (Figure SA). Assigned molecular formulas revealed that these compounds had 4–21 fluorines and that 40 of the detected features had the same number of fluorines as 6:2 FTS (13 fluorines). Van Krevelen diagrams (Figure SB, i.e., plots of atomic H:C and O:C ratios) evidenced molecules related by an apparent oxidation step as shown by the numerous compounds with identical fluorine counts and H:C ratios, but different O:C ratios. Similarly, plotting the  $\text{CF}_2$ -normalized Kendrick mass defect and the Kendrick mass (Figure SC) showed characteristic periodic relationships between the detected compounds. As an orthogonal measure of the relationship among the detected

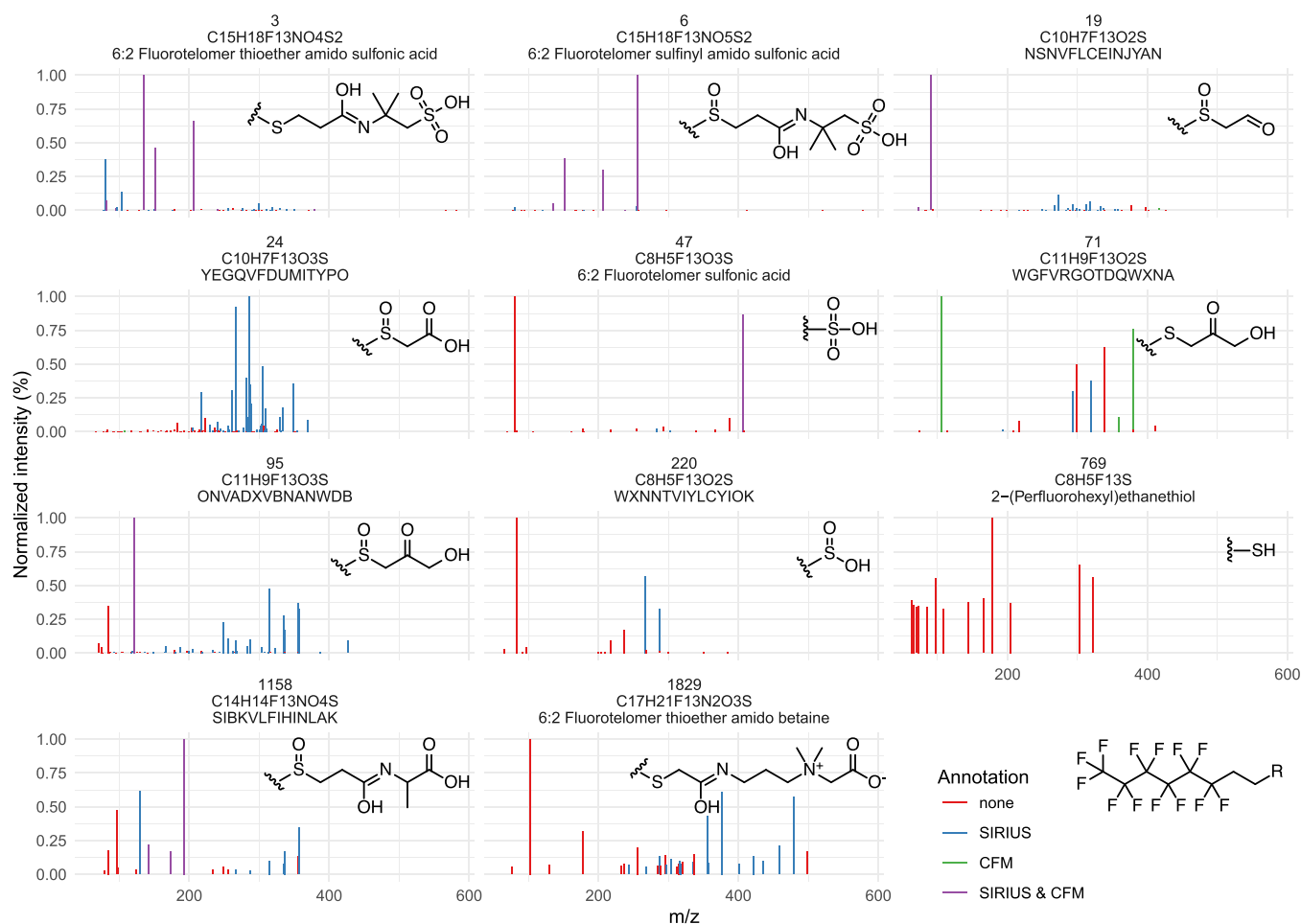


**Figure 7.** MS/MS spectra for annotated features detected in AFFF-impacted surface water. Panels are labeled by feature number, molecular formula, and name or InChi Key in order of decreasing maximum area. Inset structure fragments depict substituents relative to the 6:2 fluorotelomer backbone depicted at the bottom right. Mass spectral peaks are colored according to the degree of molecular or structural annotation. Where a detected  $m/z$  was found as a member of a fragment tree constructed by SIRIUS, peaks are colored blue. Where CFM predicted a fragment ion structure matching an observed  $m/z$  value, the peak is colored green. Where both SIRIUS and CFM provided annotations, peaks are colored purple. Finally, peaks with no annotation are colored red.

compounds, we constructed fragment trees using SIRIUS for each compound and compared overlap in fragment ion molecular formulas. Figure 5D depicts the fragment ion molecular network for the detected compounds and reveals relationships between compounds by conserved fragment ion molecular formulas among the detected compounds.

To empirically extract compounds for further analysis, we focused on those that exhibited large peak areas, predicted environmental transformations in the underlying reaction database, and conserved MS/MS fragment ions. Therefore, we further constrained the compound list to those with node distances, in either the reaction network or the fragment ion network, less than four nodes from the highest-intensity compound (i.e., number 3). This additional filtering step reduced the total number of candidate PFASs to 24. Finally, putative structure assignments made through CFM *in silico* spectral library searching showed a preponderance of putative structure assignments containing sulfur-based 6:2 fluorotelomer substructures, including the highest-intensity detected compound. Therefore, we additionally filtered compounds to consider only those where the top-ranked putative structure assignment contained a sulfur atom linked by an ethyl group to a

C<sub>6</sub>-perfluorinated alkyl chain, resulting in the 11 putative annotations depicted in Figures 6 and 7.

Figure 6 depicts the molecular network of the 11 compounds passing the described filtering steps and representative tentatively assigned structures and transformation reaction identifiers. Nodes depicted in Figure 6 represent PFASs returned from the database search that were either detected in a sample (orange points) or connected to a detected compound by a predicted transformation relationship, but were not detected experimentally (green points). Detected features were largely connected by biotransformation rules, reflecting likely in-stream biodegradation. Table S3 lists the molecular identifiers and reaction identifiers for relationships depicted in Figure 6. A description of the biotransformation rules annotated in Figure 6 can be found in Table S4.

Compound annotations with extant EPA Chemistry Dashboard<sup>27</sup> records, those with chemical names in Figure 7, totaled five structures. On the basis of this approach, the highest-intensity compound (compound 3) was tentatively identified as 6:2 fluorotelomer thioether amido sulfonic acid (6:2 FTSAS), which is a fluorinated sulfonic acid surfactant known to be an AFFF component.<sup>28</sup> The 1977 patent disclosing the use of 6:2 FTSAS as a surfactant<sup>29</sup> indicates synthesis from 2-

(perfluorohexyl)ethanethiol, which was detected as compound 769. Consistent with previous reports characterizing FTSAS-based AFFF, the sulfoxide oxidation product of 6:2 FTSAS was detected in our analysis (compound 6).<sup>28,30</sup> While 6:2 FTSAS sulfoxide may occur as an impurity in AFFF, it has also been reported as an intermediate biodegradation product of 6:2 FTSAS, along with 6:2 FTS (compound 47), in aerobic soil mesocosm experiments seeded with AFFF.<sup>31</sup> The ratio of 6:2 FTSAS to 6:2 FTSAS sulfoxide peak areas decreased from >7 in the sample nearest the AFFF release to approximately 1.5–2.3 at a distance of ~850 m downstream, indicating potential in-stream oxidation of 6:2 FTSAS to 6:2 FTSAS sulfoxide, consistent with the known biodegradation pathway of 6:2 FTSAS. Most of the other annotated features were apparent oxidation products or hydrolysis products of 6:2 FTSAS, including 6:2 FTS (see Figure 6 for predicted transformation relationships). Several of the tentatively identified transformation products we report here have been noted to occur during wastewater treatment of concentrated wastes containing AFFF.<sup>32</sup> However, to the best of our knowledge, this report represents the first identification of these compounds in the ambient environment. Compounds detected in our analysis that, to the best of our knowledge, have not been previously identified in environmental media are highlighted in Figure 6.

Confidence in assigned structure annotations varied according to the level of molecular or structural annotation achieved and the context of the environmental compartment under consideration. In the example presented here, where AFFF is known to be applied, structure annotations for compounds known to be active ingredients in AFFF are regarded as highly probable. However, it is important to note that our analysis had no *a priori* assumption that identified molecules must have a known use as an AFFF ingredient to be considered as potential structures. This is evident in the annotation of compounds representing likely transformation products of 6:2 FTSAS, which would not appear in common screening databases compiled from commercial PFAS compounds but were present in our transformation product database and linked to 6:2 FTSAS by either a mechanistically plausible environmental transformation pathway or shared fragment ions.

Annotation of tandem mass spectra by computational mass spectrometry tools provides further evidence for the plausibility of proposed structures. The SIRIUS algorithm assigns fragmentation trees utilizing a logarithmized likelihood estimation method to determine probable subtree arrangements of molecular formulas assigned to intact molecular ions and associated fragment ions without attempting to assign the arrangement of elements in the molecule (i.e., operates only on the molecular formula level).<sup>33</sup> In contrast, CFM predicts ion decomposition reactions based on a machine learning algorithm and generates predicted fragment ion structures.

Figure 7 shows MS/MS spectra for the unknown PFASs with peaks colored according to annotation by SIRIUS (blue), CFM (green), SIRIUS and CFM (purple), or neither CFM nor SIRIUS (red). Annotations where a high number of fragment ion peaks and a large fraction of the total fragment ion intensity are explained by both SIRIUS and CFM should be regarded as probable structure assignments (compounds 3, 6, and 19 in Figure 7). Instances in which SIRIUS, but not CFM, provided annotation may indicate structures poorly represented among the training set of the CFM algorithm. These structure annotations should be regarded as possible structure assignments with the caveat that they are definitively members of the

sulfur-based 6:2 fluorotelomer class. In at least one instance, no or very few SIRIUS or CFM fragment ion annotations were assigned. Peaks highlighted in red in Figure 7 indicate instances in which an observed  $m/z$  could not be rationalized by either CFM or SIRIUS and may represent atypical fragmentation reactions (e.g., rearrangements) that are not easily captured by computational mass spectrometry algorithms or the presence of chimeric MS/MS spectra arising from co-isolation of unrelated yet isobaric precursor ions. These annotations are confident only at the molecular formula level as evidenced by their low mass error and the unique molecular composition of PFASs (i.e., low H counts and high F counts).

## CONCLUSIONS

Here we have described a novel online SPE–HRMS instrument platform and associated method for the high-throughput screening of trace-level PFASs in environmental waters. The realized method offers significant improvements in both the speed of analysis and sample throughput by automation of the SPE enrichment step. Additionally, limited sample handling reduced analyte losses and contamination by laboratory equipment. Compared to direct aqueous injection methods, without prior sample enrichment, this method provides higher masses on column and concurrently lower instrument detection limits. Additionally, whereas offline SPE PFAS methods utilize 0.2–1 L of sample, the method presented here requires significantly smaller sample sizes and therefore reduces constraints on the number of samples that can be taken during sampling campaigns by alleviating sample storage and transport challenges. While the method presented here focused on providing a holistic approach for suspect screening by HRMS, the developed online SPE approach could offer significant advantages for high-throughput, targeted analysis of PFASs by conventional low-resolution mass spectrometry. Furthermore, sample preparation approaches described herein may be poorly suited for samples highly contaminated with particulate matter. Therefore, additional method refinement may be necessary to expand the range of applicable environmental waters for this method. Additionally, the method described herein focused primarily on analysis of PFASs amenable to negative ionization conditions. Future work will expand the described methodology to include PFASs preferentially or exclusively amenable to positive ionization (e.g., zwitterionic or cationic PFASs).

In addition to providing a sensitive and high-throughput method for sample analysis, this method presents a novel approach for the efficient analysis of resultant HRMS data. We have demonstrated the utility of combining a highly curated PFAS suspect screening list with molecular networking and semiautomated structure annotation using advanced computational mass spectrometry tools (i.e., fragment tree generation and *in silico* MS/MS). This approach greatly improves the analyst's ability to rapidly and confidently assign tentative structure assignments to detected PFASs.

## ASSOCIATED CONTENT

### Supporting Information

The Supporting Information is available free of charge at <https://pubs.acs.org/doi/10.1021/acsestwater.0c00309>.

Compound identifiers and reaction descriptions (Tables S1–S4) (XLSX)

## AUTHOR INFORMATION

### Corresponding Authors

**Gordon J. Getzinger** – Department of Civil and Environmental Engineering and Nicholas School of the Environment, Duke University, Durham, North Carolina 27708, United States; [orcid.org/0000-0002-5628-1425](https://orcid.org/0000-0002-5628-1425); Email: [ggetzinger@exponent.com](mailto:ggetzinger@exponent.com)

**P. Lee Ferguson** – Department of Civil and Environmental Engineering and Nicholas School of the Environment, Duke University, Durham, North Carolina 27708, United States; [orcid.org/0000-0002-8367-7521](https://orcid.org/0000-0002-8367-7521); Email: [lee.ferguson@duke.edu](mailto:lee.ferguson@duke.edu)

Complete contact information is available at:  
<https://pubs.acs.org/10.1021/acsestwater.0c00309>

### Author Contributions

G.J.G. and P.L.F. conceived and designed experiments. G.J.G. performed experiments and analysis and drafted the manuscript. Both authors have approved the final draft of the manuscript.

### Notes

The authors declare no competing financial interest.

## ACKNOWLEDGMENTS

The authors acknowledge Mei Sun, Yuling Han, Yen-Ling Liu, Vivek Pulikkal, Samonty Das, Kaitlynn Bryan-Scaggs, Ziona Bates-Norris, Dave Tilley, and Thuy Le for planning and executing surface water sampling. This work was supported by funding from the North Carolina Per- and Polyfluoroalkyl Substances Testing Network (<https://ncpfastnetwork.com>), the Michael and Annie Falk Foundation, and the NIHES HHEAR program (U2CES030851, HHEAR: Duke Environmental Analysis Laboratory).

## REFERENCES

- (1) Glüge, J.; Scheringer, M.; Cousins, I. T.; DeWitt, J. C.; Goldenman, G.; Herzke, D.; Lohmann, R.; Ng, C. A.; Trier, X.; Wang, Z. An overview of the uses of per- and polyfluoroalkyl substances (PFAS). *Environmental Science: Processes & Impacts* **2020**, *22* (12), 2345–2373.
- (2) U.S. Environmental Protection Agency. The Third Unregulated Contaminant Monitoring Rule (UCMR 3). Fact Sheet for Assessment Monitoring of List-1 Contaminants. <https://www.epa.gov/sites/production/files/2016-05/documents/ucmr3-factsheet-list1.pdf> (accessed 2020-12-24).
- (3) Rahman, M. F.; Peldszus, S.; Anderson, W. B. Behaviour and fate of perfluoroalkyl and polyfluoroalkyl substances (PFASs) in drinking water treatment: A review. *Water Res.* **2014**, *50*, 318–340.
- (4) Wang, Z.; DeWitt, J. C.; Higgins, C. P.; Cousins, I. T. A Never-Ending Story of Per- and Polyfluoroalkyl Substances (PFASs)? *Environ. Sci. Technol.* **2017**, *51* (5), 2508–2518.
- (5) McCord, J.; Strynar, M. Identification of Per- and Polyfluoroalkyl Substances in the Cape Fear River by High Resolution Mass Spectrometry and Nontargeted Screening. *Environ. Sci. Technol.* **2019**, *53* (9), 4717–4727.
- (6) Sun, M.; Arevalo, E.; Strynar, M.; Lindstrom, A.; Richardson, M.; Kearns, B.; Pickett, A.; Smith, C.; Knappe, D. R. U. Legacy and Emerging Perfluoroalkyl Substances Are Important Drinking Water Contaminants in the Cape Fear River Watershed of North Carolina. *Environ. Sci. Technol. Lett.* **2016**, *3* (12), 415–419.
- (7) van Leeuwen, S. P. J.; de Boer, J. Extraction and clean-up strategies for the analysis of poly- and perfluoroalkyl substances in environmental and human matrices. *J. Chromatogr. A* **2007**, *1153* (1–2), 172–185.
- (8) de Voogt, P.; Saez, M. Analytical chemistry of perfluoroalkylated substances. *TrAC, Trends Anal. Chem.* **2006**, *25* (4), 326–342.
- (9) Strynar, M.; Dagnino, S.; McMahan, R.; Liang, S.; Lindstrom, A.; Andersen, E.; McMillan, L.; Thurman, M.; Ferrer, I.; Ball, C. Identification of Novel Perfluoroalkyl Ether Carboxylic Acids (PFECAs) and Sulfonic Acids (PFESAs) in Natural Waters Using Accurate Mass Time-of-Flight Mass Spectrometry (TOFMS). *Environ. Sci. Technol.* **2015**, *49* (19), 11622–11630.
- (10) Dimzon, I. K.; Trier, X.; Froemel, T.; Helmus, R.; Knepper, T. P.; de Voogt, P. High Resolution Mass Spectrometry of Polyfluorinated Polyether-Based Formulation. *J. Am. Soc. Mass Spectrom.* **2016**, *27* (2), 309–318.
- (11) Liu, Y.; Dos Santos Pereira, A.; Martin, J. W. Discovery of C5–C17 poly- and perfluoroalkyl substances in water by in-line SPE-HPLC-Orbitrap with in-source fragmentation flagging. *Anal. Chem.* **2015**, *87* (8), 4260–8.
- (12) Myers, A. L.; Jobst, K. J.; Mabury, S. A.; Reiner, E. J. Using mass defect plots as a discovery tool to identify novel fluoropolymer thermal decomposition products. *J. Mass Spectrom.* **2014**, *49* (4), 291–296.
- (13) Getzinger, G. J.; Ferguson, P. L. Illuminating the exposome with high-resolution accurate-mass mass spectrometry and nontargeted analysis. *Current Opinion in Environmental Science & Health* **2020**, *15*, 49–56.
- (14) Koelmel, J. P.; Paige, M. K.; Aristizabal-Henao, J. J.; Robey, N. M.; Nason, S. L.; Stelben, P. J.; Li, Y.; Kroeger, N. M.; Napolitano, M. P.; Savvaides, T.; Vasiliou, V.; Rostkowski, P.; Garrett, T. J.; Lin, E.; Deigl, C.; Jobst, K.; Townsend, T. G.; Godri Pollitt, K. J.; Bowden, J. A. Toward Comprehensive Per- and Polyfluoroalkyl Substances Annotation Using FluoroMatch Software and Intelligent High-Resolution Tandem Mass Spectrometry Acquisition. *Anal. Chem.* **2020**, *92* (16), 11186–11194.
- (15) Getzinger, G. J.; Higgins, C. P.; Ferguson, P. L. Structure Database and In Silico Spectral Library for Comprehensive Suspect Screening of Per- and Polyfluoroalkyl Substances (PFASs) in Environmental Media by High-resolution Mass Spectrometry. *Anal. Chem.* **2021**, *93* (5), 2820–2827.
- (16) Buseti, F.; Backe, W. J.; Bendixen, N.; Maier, U.; Place, B.; Giger, W.; Field, J. A. Trace analysis of environmental matrices by large-volume injection and liquid chromatography–mass spectrometry. *Bioanal. Chem.* **2012**, *402* (1), 175–186.
- (17) Rice, N. M.; Irving, H. M. N. H.; Leonard, M. A. Nomenclature for liquid-liquid distribution (solvent extraction) (IUPAC Recommendations 1993). *Pure Appl. Chem.* **1993**, *65* (11), 2373–2396.
- (18) Woudneh, M. B.; Chandramouli, B.; Hamilton, C.; Grace, R. Effect of Sample Storage on the Quantitative Determination of 29 PFAS: Observation of Analyte Interconversions during Storage. *Environ. Sci. Technol.* **2019**, *53* (21), 12576–12585.
- (19) Pan, Y.; Wang, J.; Yeung, L. W. Y.; Wei, S.; Dai, J. Analysis of emerging per- and polyfluoroalkyl substances: Progress and current issues. *TrAC, Trends Anal. Chem.* **2020**, *124*, 115481.
- (20) Barreca, S.; Busetto, M.; Vitelli, M.; Colzani, L.; Clerici, L.; Dellavedova, P. Online solid-phase extraction LC-MS/MS: a rapid and valid method for the determination of perfluorinated compounds at sub ng-L-1 level in natural water. *J. Chem.* **2018**, *2018*, 3780825.
- (21) Sanan, T.; Magnuson, M. Analysis of per- and polyfluorinated alkyl substances in sub-sampled water matrices with online solid phase extraction/isotope tandem mass spectrometry. *J. Chromatogr. A* **2020**, *1626*, 461324.
- (22) Zhong, M.; Wang, T.; Qi, C.; Peng, G.; Lu, M.; Huang, J.; Blaney, L.; Yu, G. Automated online solid-phase extraction liquid chromatography tandem mass spectrometry investigation for simultaneous quantification of per- and polyfluoroalkyl substances, pharmaceuticals and personal care products, and organophosphorus flame retardants in environmental waters. *J. Chromatogr. A* **2019**, *1602*, 350–358.
- (23) Allen, F.; Greiner, R.; Wishart, D. Competitive fragmentation modeling of ESI-MS/MS spectra for putative metabolite identification. *Metabolomics* **2015**, *11* (1), 98–110.
- (24) Rasche, F.; Svatoš, A.; Maddula, R. K.; Böttcher, C.; Böcker, S. Computing Fragmentation Trees from Tandem Mass Spectrometry Data. *Anal. Chem.* **2011**, *83* (4), 1243–1251.

- (25) Backe, W. J.; Day, T. C.; Field, J. A. Zwitterionic, Cationic, and Anionic Fluorinated Chemicals in Aqueous Film Forming Foam Formulations and Groundwater from U.S. Military Bases by Non-aqueous Large-Volume Injection HPLC-MS/MS. *Environ. Sci. Technol.* **2013**, *47* (10), 5226–5234.
- (26) Getzinger, G. J. H.; Higgins, C. P.; Ferguson, P. Lee, Structure Database and In Silico Spectral Library for Comprehensive Suspect Screening of Per- and Polyfluoroalkyl Substances (PFASs) in Environmental Media by High-resolution Mass Spectrometry. *Anal. Chem.* **2021**, *93* (5), 2820–2827.
- (27) Williams, A. J.; Grulke, C. M.; Edwards, J.; McEachran, A. D.; Mansouri, K.; Baker, N. C.; Patlewicz, G.; Shah, I.; Wambaugh, J. F.; Judson, R. S.; Richard, A. M. The CompTox Chemistry Dashboard: a community data resource for environmental chemistry. *J. Cheminf.* **2017**, *9* (1), 61.
- (28) D'Agostino, L. A.; Mabury, S. A. Identification of Novel Fluorinated Surfactants in Aqueous Film Forming Foams and Commercial Surfactant Concentrates. *Environ. Sci. Technol.* **2014**, *48* (1), 121–129.
- (29) Dear, R. E. A.; Kleiner, E. K. Fluorinated sulfonic acids and derivatives thereof. US4014926A, 1977.
- (30) Weiner, B.; Yeung, L. W. Y.; Marchington, E. B.; D'Agostino, L. A.; Mabury, S. A. Organic fluorine content in aqueous film forming foams (AFFFs) and biodegradation of the foam component 6:2 fluorotelomermercaptoalkylamido sulfonate (6:2 FTSAS). *Environ. Chem.* **2013**, *10* (6), 486–493.
- (31) Harding-Marjanovic, K. C.; Houtz, E. F.; Yi, S.; Field, J. A.; Sedlak, D. L.; Alvarez-Cohen, L. Aerobic Biotransformation of Fluorotelomer Thioether Amido Sulfonate (Lodyne) in AFFF-Amended Microcosms. *Environ. Sci. Technol.* **2015**, *49* (13), 7666–7674.
- (32) Houtz, E.; Wang, M.; Park, J.-S. Identification and Fate of Aqueous Film Forming Foam Derived Per- and Polyfluoroalkyl Substances in a Wastewater Treatment Plant. *Environ. Sci. Technol.* **2018**, *52* (22), 13212–13221.
- (33) Dührkop, K.; Scheubert, K.; Böcker, S. Molecular Formula Identification with SIRIUS. *Metabolites* **2013**, *3* (2), 506–516.